

International Journal of Current Bio-Medical Engineering (IJCBE) Volume 3, Issue 1, January – February (2025)

RESEARCH ARTICLE

BON-VNET: SEGMENTATION OF BONE FRACTURE IN CT IMAGES WITH HOG FEATURES BASED DEEP V-NETWORK

Rajesh Thangaraj 1,* and S. Sony Helen 2

*Corresponding e-mail: tnanjilrajesh@gmail.com

Abstract - Proximal humeral fractures are common injuries, especially in youngsters and the elderly, and usually correspond to 5-6% of all fractures. There has been a general increase in upper extremity fractures in children. Detecting PHF is the time-consuming process of manual diagnosis by professionals using X-ray images. In this paper, a novel deep learning-based BON-VNET model is proposed for the detection of fracture in bones. Initially, the input CT image is pre-processed utilizing adaptive bilateral filter. Then, the pre-processed images are segmented using V-Net segmentation model. Afterward the segmented images are fed as an input the HOG based feature extraction phase for extracting the relevant features. Finally, the machine learning (ML) based ANFIS approach is employed for the classification of PHF images. From the trail result, the proposed BON-VNET model achieves 99.77% of accuracy rate, which is more than that of the conventional DL networks. Proposed BON-VNET model exhibits an overall accuracy improvement of 13.83%, 8.82%, and 16.95% compared to InceptionV3 Near classification and SVM, respectively.

Keywords – adaptive bilateral filter, V-Net, Deep learning, Machine Learning.

1. INTRODUCTION

ISSN: xxxx-xxxx

Proximal humerus fractures are recognized as quintessential osteoporotic injuries, commonly afflict the elderly populace. These fractures encompass damage to various regions of the PH, including the greater tuberosity (GT), lower tuberosity, anatomical neck, or surgical neck [1-2]. The proximal humerus, situated in the upper extremity, serves as a crucial component of the upper arm bone [3]. However, managing these fractures presents a challenge, attributable to factors such as inconsistent classification systems, lack of consensus regarding surgical indications, and the potential for difficult-to-treat complications [4]. Treatment decisions for proximal humerus fractures must carefully consider the specific anatomical characteristics of the fracture, the presence of concurrent soft tissue injuries, and other individual factors, with options ranging from conservative approaches to surgical interventions [5].

The integrity of bones is paramount for facilitating human mobility and overall functionality. Surgical intervention is typically favoured for fractures involving significant tuberosity displacement, as this mitigates the risk of further displacement and subsequent functional impairment. Orthopaedic specialists rely on imaging modalities like X-rays and CT scans [6] to diagnose and assess the extent of proximal humerus fractures [7]. Emerging technologies, such as artificial intelligence (AI), Deep Learning (DL) [8] hold promise in enhancing the diagnostic accuracy of proximal humerus fractures. AI [9] algorithms trained on shoulder CT images can accurately identify and classify these fractures, offering a potential solution to the shortage of professionals available to interpret such scans promptly [10-11]. Despite the diagnostic potential of CT imaging, the timely analysis of scans remains a challenge due to the limited availability of skilled radiologists. To overcome these problems, a novel DL-based BON-VNET model is proposed for the detection of fracture in bone. The main contribution of the proposed work is organized as follows

- Initially, the input CT image is pre-processed utilizing adaptive bilateral filter to remove the noise and enhance the quality of image.
- Then, the images are segmented using V-Net segmentation model. Afterward the segmented images are fed as an input the HOG based feature extraction phase for extracting the relevant features.
- Finally, the ML based ANFIS approach is employed for the classification of PHF images.

The remainder of the research paper is structured as follows: Section 2 offers a list and summary of relevant works. Section 3 delves into the detailed explanation of the proposed deep learning method for identifying and categorizing proximal humerus fractures. The experimental findings and ensuing discussion are presented in Section 4.

¹ Professor, Department of Electronics and Communication Engineering, PSN College of Engineering and Technology, Tirunelveli, Tamil Nadu, India

² Research Scholar, Department of Computer Science and Engineering, Anna University, Chennai, Tamil Nadu, India

Finally, Section 5 concludes the paper and outlines avenues for future research.

2. LITERATURE SURVEY

In 2020 Tanzi, L et al., [12] suggests employing a multistage DL approach to identify proximal femoral X-ray images. This involves using a tailored InceptionV3 CNN and a multistage design consisting of a cascade of CNN. The experiment achieved an average accuracy of 0.86 in classifying hip fractures (HF).

In 2021 Smith, J et al., [13] suggested categorization of PHF using the Neer method could potentially be improved by incorporating three-dimensionally printed models. Kappa values (k), percentage agreements, and 95% confidence intervals were employed to measure both interobserver and interobserver agreements.

In 2021 Askittou, S et al., [14] Suggested the examination of the consistency among different observers and within the same observer regarding the morphological Mutch categorization for fragments in the GT in PHF, the number of fragments, utilizing three distinct imaging modalities. The findings reveal that the developed model achieves 67% agreement in 2-D or 3-D CT imaging.

In 2022 Foruria, A.M et al., [15] designed the Mayo-Fundacion Jimenez Daz (FJD) for classification of PHF. The classification encompasses seven typical fracture patterns. Interobserver agreement for X-rays averaged 69%, while for CT scans it achieves 81%. The anteroposterior X-ray used for analysis was obtained in internal rotation rather than the scapular plane.

In 2022 Dipnall, J.F et al., [16] presents a method for diagnosing PHF using ML multiclass classification techniques. This approach utilizes standard unstructured X-ray and CT scan reports along with patient data processed through ML and BERT algorithms. The performance of various statistical ML algorithms was found to be

commendable, with BERT models achieving an accuracy rate of 61%.

In 2023 Ripoll, T et al., [17] suggested a computerized system to accurately measure the uniform and reliable 3D spatial displacements of PHF. This system utilizes the Neer classification method for 3D measurement. It enables precise measurement of the displacements of fracture fragments in PHFs using a three-dimensional computerized approach. The analysis focuses solely on the four primary fragments, excluding smaller fragments. The experiment yielded a 91% success rate.

In 2023 Cangöz G.B. and Güney S [18] introduces traditional methods of data augmentation for detecting long bone fractures. It utilizes the Inception-v3 network and Support Vector Machines (SVMs) to classify images and identify fractures. SVM serves as the classifier, while Transfer Learning is applied to extract features from both original and augmented datasets. The experiment yields an 84.5% accuracy rate in long bone fracture detection.

From the above study, current methods for categorizing and detecting bone fractures demonstrate inadequate accuracy. To overcome these issues, this study presents a newly developed model aimed at identifying and categorizing PHF based on CT data. One of the challenging aspects in the process of detecting and segmenting PHF involves removing extraneous features and determining crucial ones.

3. PROPOSED METHOD

In this paper, a novel DL-based BON-VNET model is proposed for the detection of fracture in bones. The input image is pre-processed utilizing adaptive bilateral filter. Then, the images are segmented using V-Net segmentation model. Afterward the segmented images are fed as an input the HOG based feature extraction phase for extracting the relevant features. Finally, the ML based ANFIS approach is employed for the classification of PHF images. Figure 1 shows the proposed BON-VNET methodology.

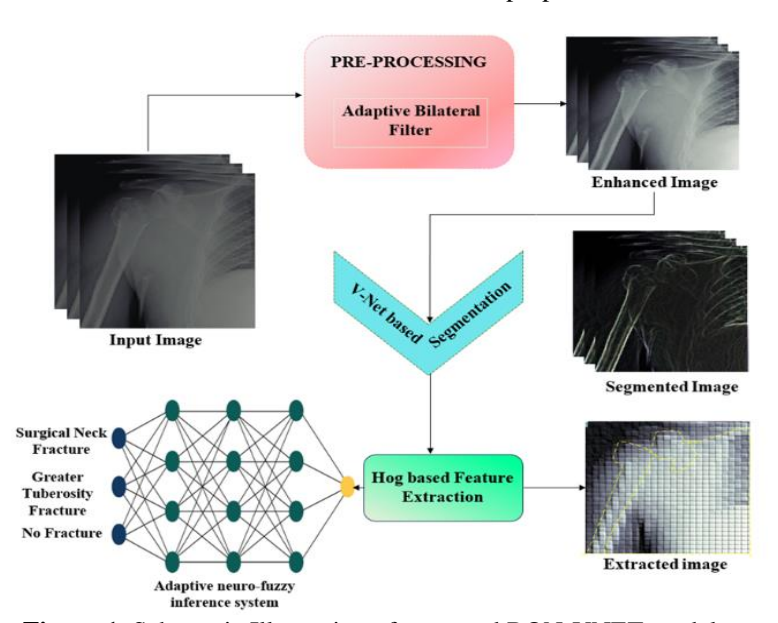


Figure 1. Schematic Illustration of proposed BON-VNET model

3.1. Adaptive Bilateral Filter

By allowing pixels to contribute selectively to the scaled average, the bilateral filter effectively reduces noise in images while maintaining edge details. The bilateral filter yields ideal results where pixels on one side of the border influence the modified pixel value due to bilateral effects, resulting in smooth images with important data, equation (1).

$$\begin{split} z_{(c,d)} &= \mathcal{N}_{gh}(\textbf{o},\textbf{I}) \sum_{\textbf{x}=-3\sigma}^{3\sigma} \delta_{gh}\left(c,d,i,j\right) \mathcal{I}(c+i,d+j) \quad \quad (1) \end{split}$$
 The normalization bilateral filter, represented by \mathcal{N}_{gh} ,

utilizes δ_{gh} to signify the dimensions for individual pixels within the filter space. It smooths the function $f_3(g,h)$ to estimate the Gaussian size, incorporating a Gaussian weight factor via a visual inclusion factor for adaptable pixel value selection in the scaled overall form (c, d, i, j), equation (2).

$$\delta_{gh}(c,d,i,j) = \mathfrak{f}_{\mathfrak{F}}(g,h) \tag{2}$$

 \mathcal{N}_{gh} is serving as a normalization factor Which is computed by inversing the total dimensions.

The bilateral filter functions as a non-linear noise reduction filter. Outcomes are influenced by filtering and pixel-level factors, equation (3) is utilized to determine the range of filter pixels, considering their distance from the central point.

$$g(j-1) = \frac{1}{2}Q^{-(j-1)^{\Lambda}2(\frac{1}{2\tau})}$$
(3)

In the equation provided, the pixel value of the image position is denoted by j-1, corresponds to the spatial function represented by 2τ.

3.2. Segmentation

The Volumetric Convolutional Net (V-Net) is a progressive DL structure crafted for image segmentation. Comprising a symmetrical five-layer network, it incorporates an encoder for extracting spatial features from images, a decoder for constructing segmentation graphs based on encoded features, and a skip connection framework that merges positional data from the encoding path with contextual data from the decoding path. This integration aims to address the absence of edge features and spatial data during the decoding phase. Additionally, residual units are incorporated into the network to mitigate the loss of network gradient, and the assessment is articulated through equation

$$g_{B} = g_{c} + \sum_{m=1}^{B-1} F(g_{m}, k_{m})$$
(4)

This design helps the network retain fine-grained spatial details during the segmentation process. In the given equation, F represents the residual value, g_m stands for the input feature image, and k_m denotes the size associated with the residual units.

The V-Net employs convolutional and transpose convolutional layers for up sampling. The number of channels in the feature map is ultimately adjusted through a 1*1 convolution in the last layer, and the final probability map is generated using a sigmoid function. To prevent overfitting, a dropout layer is added at the end of each layer's residual unit.

3.3. HOG based Feature Extraction

Histogram of Oriented Gradients (HOG) is a powerful feature descriptor commonly used in computer vision tasks, particularly in object detection. It works by describing the local object appearance and shape within an image based on the distribution of gradient orientations. The first step is to calculate the gradient values of the image. These filters help to capture the changes in intensity or color across the image, which are indicative of edges and other important features, equation (5) and (6).

$$\begin{aligned}
\dot{a}_z &= [-1 \ 0 \ 1] \\
a_x &= \begin{bmatrix} 1 \\ 0 \\ 1 \end{bmatrix}
\end{aligned} (5)$$

If the object image is 1, the factor z and x is obtains utilizing the below convolution operation, equation (7) and

$$I_z = I_z \times A_z \tag{7}$$

$$I_x = I_x \times A_x \tag{8}$$

From the above evaluation the gradient of magnitude is calculated utilizing the equation (9).

$$|g| = \sqrt{I_z^2 + I_x^2} \tag{9}$$

These blocks can overlap with each other, allowing for better coverage of the image and capturing more spatial information. Finally, normalization is applied to the feature vectors within each block to account for variations in lighting and contrast across different regions of the image. This normalization step helps to make the descriptor more robust to changes in illumination and improves its discriminative power. By capturing the distribution of gradients in different spatial regions of the image, the HOG descriptor provides a compact and informative representation of local object appearance and shape, making it well-suited for computer vision applications.

3.4. Classification

The ANFIS utilizes an adaptive system framework integrating a fuzzy Sugeno model, enhancing its learning and adaptability. This framework reduces reliance on expert knowledge, making ANFIS modeling more systematic, equation (10) and (11).

Rule 1: If (b is
$$t_1$$
) and (d is n_1) then ($f_1 = z_1b + x_1d + s_1$)

(10)

Rule 2: If (b is t_2) and (d is n_2) then ($f_2 = z_2b + x_2d + s_2$)

(11)

From the equation, u are the inputs, t_1 and n_1 are the fuzzy sets, f_1 be the outputs within the fuzzy region specified by the fuzzy rule z_1 , x_2 , and s_1 are the design factors that are determined during the training process. The output of layer 1 is determined by the fuzzy membership class of the components provided, equation (12) and (13).

$$p_0^1 = A_b(b)$$
 (12)
$$p_0^1 = A_{n_{0-2}}(d)$$
 (13)

$$p_0^1 = A_{n_{2-2}}(d) \tag{13}$$

From the equation, $A_b(b)$ and $A_{n_{0-2}}(d)$ are adopt fuzzy membership function. The nodes in the second layer remain fixed and operate as fundamental multipliers based on their respective labels. Below is an illustration of the outputs from this layer, equation (14).

$$p_0^1 = A_b(b)A_{n_0-2}(d) (14)$$

Additionally, the nodes located in the third tier are stationary nodes, denoted by the letter N alongside their designation, indicating their role in standardizing, equation (15).

$$p_0^3 = \frac{t_b}{t_1 + t_1} \tag{15}$$

Nodes with adaptability can be located within the fourth layer, where each node's output in every layer is the product of multiplying the first-order polynomial by the normalized firing strength and the model's overall output as depicted in equation (16).

$$p_0^5 = \frac{\sum_{i=1}^2 t_b \lambda_b}{t_1 + t_1} \tag{16}$$

The ANFIS architecture incorporates two adaptive layers, namely the initial and fourth layers. Within the initial layer, there are three adjustable parameters $(\alpha_n, \beta_n, \gamma_n)$ associated with input membership functions, known as premise parameters.

4. RESULTS AND DISCUSSION

The effectiveness of the suggested BON-VNET network is evaluated in using the MDCT dataset [19]. This dataset is employed to gather the input CT images, which are subsequently pre-processed to prepare them for further analysis.

Input	Pre-processing image	Feature Extraction	Classification
			Surgical neck
9	97	3	Tuberosity
			Normal
			Surgical neck

Figure 2. The proposed BON-VNET Model's outcomes from experiments

Figure 2 illustrates the results of the proposed BON-VNET model's visualization. Initially, the input CT images undergo denoising in column 1 to remove distortions and improve image quality, as shown in column 2. These denoised images are then processed for feature extraction in column 3. Subsequently, the cleaned and detected images are inputted into the ANFIS model to classify proximal humerus fractures, including tuberosity fracture, surgical neck fracture, and normal cases, as depicted in column 4.

4.1. Performance Analysis

The effectiveness and performance of the suggested BON-VNET model were verified using evaluation metrics. True Positive (True P), True Negative (True N), False Positive (False P), and False Negative (FalseN) are the four main and essential metrics that are frequently employed to determine performance, equation (17), (18), (19) and (20).

$$Accuracy = \frac{\text{True P+True N}}{\text{True P+True N+False P+False N}} \times 100$$
 (17)

$$Precision = \frac{\text{True P}}{\text{True P+False P}}$$

$$Recall = \frac{\text{True P+False P}}{\text{True P+False N}}$$
(18)

$$Recall = \frac{\text{True P}}{\text{True PLEstee N}} \tag{19}$$

$$F1 - Score = \frac{2}{\frac{1}{(Perall)} + \frac{1}{(Precision)}} \tag{20}$$

Table 1. Analysis of Proposed Method Statistics

Classes	Accu	Precisi	Recal	Specifi	F1
	racy	on	l	city	score
Tuberosit	99.81	99.13	97.98	97.02	98.47
у					
Normal	99.76	98.89	97.88	95.78	98.55
Surgical	99.87	98.95	96.11	96.92	97.23
Neck					

The following Table 1 illustrates the effectiveness of the proposed BON-VNET model to classify the different Proximal humerus cases. A 99.77% accuracy rate is achieved by the proposed model.

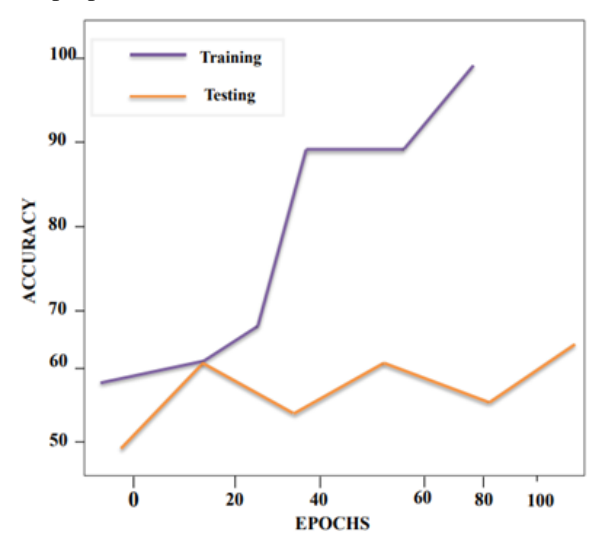


Figure 3. Accuracy of proposed BON-VNET model

Figure 3 accuracy graph was generated by utilizing 100 epochs and observing an accuracy trend. As the number of epochs rises, the accuracy of the suggested model is increases.

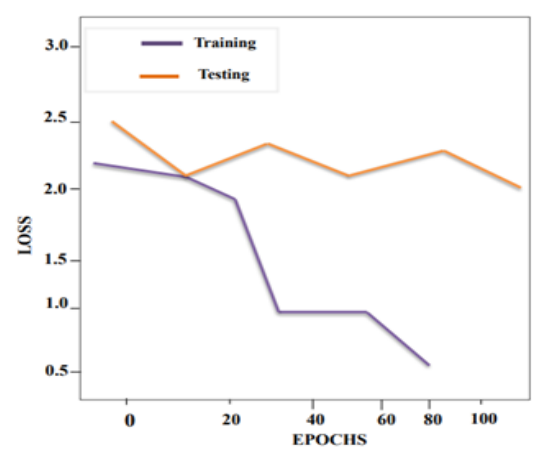


Figure 4. Loss of proposed BON-VNET model

Figure 4, which displays the epochs and loss range, shows that increasing the epochs reduces the loss of the suggested model. After 100 training epochs, the suggested model demonstrated a 99.77% detection accuracy with a low

4.2. Comparative Analysis

The efficacy of the suggested approach yields highly accurate results. The suggested Networks underwent competency testing using DL algorithms: Random Forest, and SVM. The proposed model accuracy is 99.77%, which is more than that of the conventional DL networks.

Table 2. Comparison of multiple networks

Networ ks	Accura cy	Precisi on	Reca II	Specifici ty	F1 scor
SVM	99.29	97.15	96.4 0	95.74	96.3 4
Rando m Forest	99.27	98.18	97.3 4	96.30	96.2 7
propose d ANFIS	99.77	98.29	97.2 1	97.72	97.4 4

Table 3. Compare the accuracy of existing models and the proposed model

Author	Methods	Accuracy
Tanzi, L et al.,	InceptionV3	86%
[21]	CNN	
Ripoll, T et al.,	Neer	91%
[29]	classification	
Cangöz G.B. and	SVM	84.5%
Güney S [30]		
Proposed Model	ANFIS	99.77%

The trial period for testing images collected from the dataset has been set up to evaluate different approaches' effectiveness, as detailed in Table 2. Various measures are employed to compare existing models with high classification accuracy. Proposed model exhibits an overall accuracy improvement of 13.83%, 8.82%, and 16.95% compared to InceptionV3 Near classification and SVM, respectively. The proposed network demonstrates more efficient data processing compared to previous networks. Table 3 clearly shows that our innovative network surpasses current methods.

CONCLUSION

In this paper, a novel DL-based BON-VNET model is suggested for the detection of fracture in bones. The input image is pre-processed utilizing adaptive bilateral filter. Then, images are segmented using V-Net segmentation model. Afterward the segmented images are fed as an input the HOG based feature extraction phase for extracting the relevant features. Finally, the ML based ANFIS approach is employed for the classification of PHF images. From the trail result, the proposed model achieves 99.77% of accuracy rate, which is more than that of the conventional DL networks.

Proposed model exhibits an overall accuracy improvement of 13.83%, 8.82%, and 16.95% compared to InceptionV3 Near classification and SVM, respectively. In the future, enhance the suggested model by integrating more sophisticated deeplearning methods to detect different types of fractures. Furthermore, different segmentation techniques could be employed to precisely locate the classified region.

CONFLICTS OF INTEREST

The authors declare that there is no conflict of interest.

FUNDING STATEMENT

Authors did not receive any funding.

ACKNOWLEDGEMENTS

The author would like to express his heartfelt gratitude to the supervisor for his guidance and unwavering support during this research for his guidance and support.

REFERENCES

- [1] P. Hadji, B. Schweikert, E. Kloppmann, P. Gille, L. Joeres, E. Toth, L. Möckel, and C. C. Glüer, "Osteoporotic fractures and subsequent fractures: imminent fracture risk from an analysis of German real-world claims data", *Archives Gynecology Obstetrics*, vol. 304, pp. 703-712, 2021. [CrossRef] [Google Scholar] [Publisher Link]
- [2] K Takayama, and H. Ito, "Turned stem tension band technique for tuberosity repair during humeral head arthroplasty for acute proximal humeral head fracture", *Seminars Arthroplasty: JSES* WB Saunders, vol. 33, no. 2, pp. 209-217, 2023. [CrossRef] [Google Scholar] [Publisher Link]
- [3] L. Zhao, Y. M. Qi, L. Yang, G. R. Wang, S. N. Zheng, Q. Wang, B. Liang, and C. Z. Jiang, "Comparison of the effects of proximal humeral internal locking system (PHILOS) alone and PHILOS combined with fibular allograft in the treatment of Neer three-or four-part proximal Humerus fractures in the elderly", *Orthopaedic Surgery*, vol. 11, no. 6, pp. 1003-1012, 2019. [CrossRef] [Google Scholar] [Publisher Link]
- [4] M. Herteleer, A. Runer, M. Remppis, J. Brouwers, F. Schneider, V. C. Panagiotopoulou, B. Grimm, C. Hengg, R. Arora, S. Nijs, and P. Varga, "Continuous Shoulder Activity Tracking after Open Reduction and Internal Fixation of Proximal Humerus Fractures", *Bioengineering*, vol. 10, no. 2, pp. 128, 2023. [CrossRef] [Google Scholar] [Publisher Link]
- [5] A. Jegatheesh, N. Kopperundevi and M. Anlin Sahaya Infant Tinu, "Brain aneurysm detection via firefly optimized spiking neural network", *Int. J. Current Bio-Medical Eng.*, vol. 01, no.01, pp. 23-29, 2023. [CrossRef] [Google Scholar] [Publisher Link]
- [6] F. N. Schmidt, M. Hahn, K. E. Stockhausen, T. Rolvien, C. Schmidt, T. Knopp, C. Schulze, K. Püschel, M. Amling, and B. Busse, "Influence of X-rays and gamma-rays on the mechanical performance of human bone factoring out the intraindividual bone structure and composition indices", *Materials Today Bio*, vol. 13, pp.100169, 2022. [CrossRef] [Google Scholar] [Publisher Link]
- [7] R. Kanthavel, R. Dhaya, and A. Ahilan, "AI-Based Efficient WUGS Network Channel Modeling and Clustered Cooperative Communication", ACM Transactions on Sensor

- *Network*s, vol. 18, no. 3, 2022. [CrossRef] [Google Scholar] [Publisher Link]
- [8] E. Fenil, G. Manogaran, G. N. Vivekananda, T. Thanjaivadivel, S. Jeeva, and A. J. C. N. Ahilan, "Real time violence detection framework for football stadium comprising of big data analysis and deep learning through bidirectional LSTM", Comput. Netw., vol. 151, pp. 191-200, 2019. [CrossRef] [Google Scholar] [Publisher Link]
- [9] R. Gogna, G. Bhabra, and C. S. Modi, "Fractures of the proximal humerus: Overview and non-surgical management", *Orthopaedics Trauma*, vol. 33, no. 5, pp. 315-321, 2019. [CrossRef] [Google Scholar] [Publisher Link]
- [10] M. Warnhoff, G. Jensen, R. O. D. Hazra, P. Theruvath, H. Lill, and A. Ellwein, "Double plating-surgical technique and good clinical results in complex and highly unstable proximal humeral fractures", *Injury*, vol. 52, no. 8, pp. 2285-2291, 2021. [CrossRef] [Google Scholar] [Publisher Link]
- [11] L. Tanzi, E. Vezzetti, R. Moreno, A. Aprato, A. Audisio, and A. Massè, "Hierarchical fracture classification of proximal femur X-Ray images using a multistage Deep Learning approach", *European J. Radiology*, vol. 133, pp. 109373, 2020. [CrossRef] [Google Scholar] [Publisher Link]
- [12] H. Bougher, P. Buttner, J. Smith, J. Banks, H. S. Na, D. Forrestal, and C. Heal, "Interobserver and intraobserver agreement of three-dimensionally printed models for the classification of proximal humeral fractures", *JSES international*, vol. 5, no. 2, pp. 198-204, 2021. [CrossRef] [Google Scholar] [Publisher Link]
- [13] S. Razaeian, S. Askittou, B. Wiese, D. Zhang, A. Harb, C. Krettek, and N. Hawi, "Inter-and intraobserver reliability of morphological Mutch classification for greater tuberosity fractures of the proximal humerus: A comparison of x-ray, two-, and three-dimensional CT imaging", *Plos one*, vol. 16, no. 11, pp. 0259646, 2021. [CrossRef] [Google Scholar] [Publisher Link]
- [14] A. M. Foruria, N. Martinez-Catalan, B. Pardos, D. Larson, J. Barlow, and J. Sanchez-Sotelo, "Classification of proximal humerus fractures according to pattern recognition is associated with high intraobserver and interobserver agreement", *JSES International*, vol. 6, no. 4, pp. 563-568, 2022. [CrossRef] [Google Scholar] [Publisher Link]
- [15] T. Ripoll, M. Chelli, T. Johnston, J. Chaoui, M. O. Gauci, H. Vasseur, S. Poltaretskyi, and P. Boileau, "Three-Dimensional Measurement of Proximal Humerus Fractures Displacement: A Computerized Analysis", J. Clinical Medicine, vol. 12, no. 12, pp. 4085, 2023. [CrossRef] [Google Scholar] [Publisher Link]
- [16] J. F. Dipnall, J. Lu, B. J. Gabbe, F. Cosic, E. Edwards, R. Page, and L. Du, "Comparison of a state-of-the-art machine and deep learning algorithms to classify proximal humeral fractures using radiology text", *European J. Radiology*, vol. 153, pp.110366, 2022. [CrossRef] [Google Scholar] [Publisher Link]
- [17] G. B. Cangöz, and S. Güney, "The Effects of the Traditional Data Augmentation Techniques on Long Bone Fracture Detection", *Bilge Int. J. Sci. Technol. Res.*, vol. 7, no. 1, pp.63-69, 2023. [CrossRef] [Google Scholar] [Publisher Link]
- [18] G. Hagleitner, P. Pichler, and F. A. Fellner, "Understanding vascular pathoanatomy: Cinematic Rendering of an abdominal aortic aneurysm treated with chimney endovascular aortic repair", *Glob Imaging Insights*, vol. 5, 2020. [CrossRef] [Google Scholar] [Publisher Link]

AUTHORS



T. Rajesh has completed B.E in ECE at M.S University in the year 2003, M.E in Applied Electronics at Anna university in the year 2006 and Ph.d in Information and Communication Engineering at Anna university during the year 2019. He is working as an Professor at PSN College of Engineering and Technology. He is having 19 years of teaching experience. His research interests are medical image Processing and wireless communication. He has published more

than 30 papers in national and international journals



S. Sony Helen is a dedicated Full-Time Research Scholar in the Department of Information and Communication Engineering at Anna University, India. With a profound interest in cutting-edge technologies, her research spans diverse areas such as Image Processing, Networking, the Internet of Things, Cloud Computing in Medical, and Cryptography. Having showcased her scholarly achievements on an international stage, Ms.

Helen has presented her research at prestigious conferences, contributing valuable insights to the academic community. Her academic journey includes roles as a Lecturer in the Department of Computer Science and Engineering at Bhajarang Engineering College, Chennai, India. Additionally, she has served as a Software Faculty for MCA, BCA, and PGDCA at the Alagappa University Study Center, India. In these capacities, she has imparted knowledge and nurtured the academic growth of her students. As a versatile developer, she specializes in diverse domains, including but not limited to Computer Networks, Medical Systems, Computer and Electrical Engineering, Neural Computing and Applications, Cluster Computing, and Image Processing. Her proficiency in these areas reflects a keen understanding of technological trends and a commitment to pushing the boundaries of innovation. Her dynamic contributions to academia and research position her as a valuable asset in the pursuit of knowledge and technological advancement. Her dedication to excellence and continuous learning underscores her commitment to making meaningful contributions to the ever-evolving landscape of information and communication engineering.

Arrived: 02.01.2025 Accepted: 05.02.2025